frontiers in Chemistry

ORIGINAL RESEARCH
published: 16 December 2021
doi: 10.3389/fchem.2021.785431

The Oxidation Cascade of a Rare Multifunctional P450 Enzyme Involved in Asperterpenoid A Biosynthesis

Hui-Yun Huang[1], Jia-Hua Huang[2], Yong-Heng Wang[1], Dan Hu[1], Yong-Jun Lu[3], Zhi-Gang She[4], Guo-Dong Chen[1], Xin-Sheng Yao[1,2] and Hao Gao[1]**

[1]Institute of Traditional Chinese Medicine and Natural Products, College of Pharmacy/Guangdong Province Key Laboratory of Pharmacodynamic Constituents of TCM and New Drugs Research, Jinan University, Guangzhou, China, [2]School of Traditional Chinese Materia Medica, Shenyang Pharmaceutical University, Shenyang, China, [3]School of Life Sciences, Sun Yat-sen University, Guangzhou, China, [4]School of Chemistry, Sun Yat-sen University, Guangzhou, China

The cytochrome P450 enzymes (P450s or CYPs) are heme-containing enzymes which catalyze a wide range of oxidation reactions in nature. In our previous study, a rare multifunctional P450 AstB was found, which can dually oxidize two methyl groups (C-19 and C-21) of preasperterpenoid A to asperterpenoid A with 3-carboxyl and 11-hydroxymethyl groups. However, the oxidation order of C-19 and C-21 catalyzed by AstB is unclear. In order to reveal this oxidation order, probable pathways catalyzed by AstB were proposed, and the oxidation order of C-19 and C-21 was obtained by quantum chemistry calculations. The potential intermediates (three new asperterpenoids D–F, **1**–**3**) were obtained through the chemical investigation on the extract of the transformant strain and chemical conversions, which were used as the standards to detect their existences in the extract of the transformant strain with HPLC-MS. Combined with the quantum chemistry calculation and the HPLC-MS analysis, the catalyzed order of AstB in asperterpenoid A biosynthesis was revealed. Furthermore, the *m*PTPB inhibition of obtained asperterpenoids was evaluated, and the results showed that 3-carboxyl and the oxidation station of C-21 would be the key factors for *m*PTPB inhibition of asperterpenoids.

Keywords: multifunctional P450s, methyl oxidation, asperterpenoids, *m*PTPB inhibition, oxidation cascade

OPEN ACCESS

Edited by:
Xiachang Wang,
Nanjing University of Chinese Medicine, China

Reviewed by:
Giovanna Di Nardo,
University of Turin, Italy
Ahmed M. Sayed,
AlMaaqal University, Iraq

****Correspondence:***
Guo-Dong Chen
chgdtong@163.com
Hao Gao
tghao@jnu.deu.cn

Specialty section:
This article was submitted to Medicinal and Pharmaceutical Chemistry, a section of the journal Frontiers in Chemistry

Received: *29 September 2021*
Accepted: *15 November 2021*
Published: *16 December 2021*

Citation:
Huang H-Y, Huang J-H, Wang Y-H, Hu D, Lu Y-J, She Z-G, Chen G-D, Yao X-S and Gao H (2021) The Oxidation Cascade of a Rare Multifunctional P450 Enzyme Involved in Asperterpenoid A Biosynthesis. Front. Chem. 9:785431. doi: 10.3389/fchem.2021.785431

INTRODUCTION

Cytochrome P450 enzymes (P450s or CYPs) are a kind of enzyme catalyzing a wide range of oxidation reactions at the specific site of molecules, which play an important role in the metabolism of organisms (Sheng et al., 2009) and the biosynthesis of natural products with potent bioactivity (Jiang et al., 2021; Lin et al., 2019). For examples, human P450c11 catalyzes the generation of cortisol (one of glucocorticoids in human organisms) from 11-deoxycortisol (Bertram et al., 2012). P450 2D6 is in charge for the transformation of codeine to morphine (one of the famous analgesics) (Kramlinger et al., 2015). TwCYP712K1 performs the three-step oxidation of fridelin to polpunonic acid in celastrol (a potent anticancer and anti-obesity natural product from *Tripterygium wilfordii* Hook. f) (Zhou et al., 2021). More and more research studies have found that some P450s can be involved in the oxidation reactions with multiple sites of molecules (Bai et al., 2020; Child et al., 2019; Erickson et al., 2007; Yanni et al., 2008; Zeng et al., 2019) and catalyze non-oxidation reactions (Bai et al., 2020; Keyler et al., 2003; Long and Dolan,

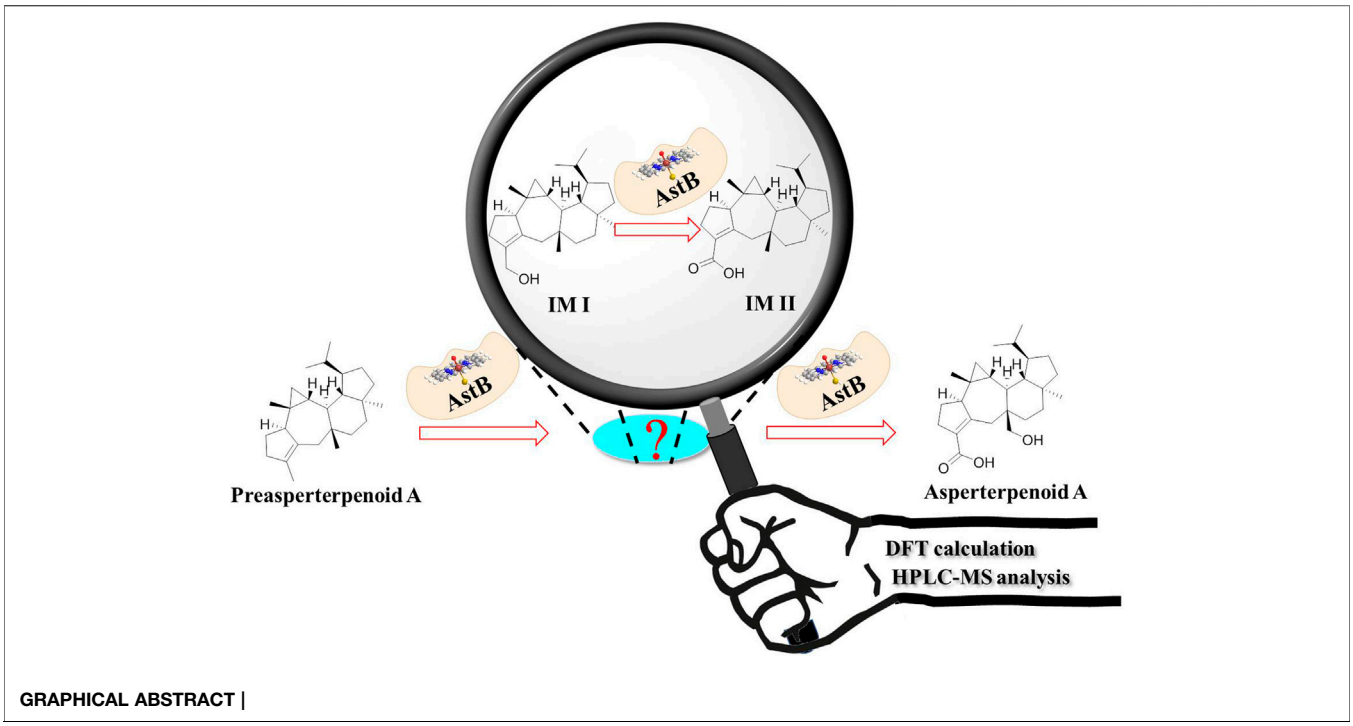

GRAPHICAL ABSTRACT |

2001; Peyronneau et al., 2012), which are classified as multifunctional P450s. In reported multifunctional P450 family, only few oxidation cascades have been demonstrated (Cochrane and Vederas, 2014; Erickson et al., 2007; Mendez et al., 2014; Moses et al., 2015; Narita et al., 2016; Zeng et al., 2019).

In our search of bioactive compounds from fungi through genome mining (Huang et al., 2019; Zhang et al., 2020), a rare oxidation multifunctional P450 AstB was found, which was solely responsible for the transformation of preasperterpenoid A to asperterpenoid A (the molecule with 3-carboxyl and 11-hydroxymethyl groups) *via* C-19 and C-21 oxidations of preasperterpenoid A (**Figure 1**). Furthermore, asperterpenoids A (IC_{50} = 2.16 μM) and B (the molecule with 3,11-dicarboxyl, IC_{50} = 2.50 μM) presented the potent inhibition against *Mycobacterium tuberculosis* protein tyrosine phosphatase B (*m*PTPB, a virulence factor secreted by *M. tuberculosis* and can facilitate the establishment of tuberculosis infection and pathogenesis) (Huang et al., 2013; Huang et al., 2019). However, the oxidation order of C-19 and C-21 catalyzed by AstB remained obscure because no intermediate in the generation of asperterpenoid A was obtained from the heterologously expressed *astBC*-harboring transformant strain (*Aspergillus oryzae*) with the previous fermentation condition (Huang et al., 2019). Therefore, the quantum chemistry calculations of the oxidation order of C-19 and C-21, the acquirements of the potential intermediates, and the HPLC-MS detection of the potential intermediates in the transformant strain were carried out. In addition, the *m*PTPB inhibition of obtained asperterpenoids was also evaluated.

MATERIALS AND METHODS

General Experimental Procedures

Methanol (MeOH) was purchased from Yuwang Industrial Co. Ltd. (Yucheng, China). Acetonitrile (MeCN) and acetone were obtained from Oceanpak Alexative Chemical Co. Ltd. (Gothenburg, Sweden). Cyclohexane and ethyl acetate (EtOAc) were analytical grade from Fine Chemical Co. Ltd. (Tianjin, China). The biochemical reagents and kits used in this study were purchased from TaKaRa Bio Inc. (Dalian, China), Thermo Fisher Scientific Inc. (Shenzhen, China), and Sangon Biotech Co. Ltd. (Shanghai, China), unless noted otherwise.

UV data, IR data, and optical rotations were, respectively, measured on the JASCO V-550 UV/vis spectrometer, JASCO FT/IR-4600 plus spectrometer, and JASCO P2000 digital polarimeter from JASCO International Co. Ltd. (Tokyo, Japan). ECD spectra were recorded in MeOH using a JASCO J-810 spectrophotometer (Jasco International Co. Ltd., Tokyo, Japan) at room temperature. The HRESIMS data were obtained on a Waters Micromass Q-TOF mass spectrometer from Waters Corporation (Milford, United States). 1D and 2D NMR spectra were recorded with the Bruker AV 600 spectrometer from Bruker BioSpin Group (Faellanden, Switzerland) using the solvent signals ($CDCl_3$: δ_H 7.26/δ_C 77.0) as the reference. Analytical HPLC was performed on a Thermo Fisher HPLC system equipped with an Ultimate 3000 pump, an Ultimate 3000 diode array detector, an Ultimate 3000 column compartment, an Ultimate 3000 autosampler (Thermo Fisher, United States), and an Alltech (Grace) 2000ES evaporative light scattering detector (Alltech, United States) using a COSMOSIL 3C18-EB column (4.6 mm i.d. × 150 mm, 3 μm) with a linear gradient of 50–100% H_2O

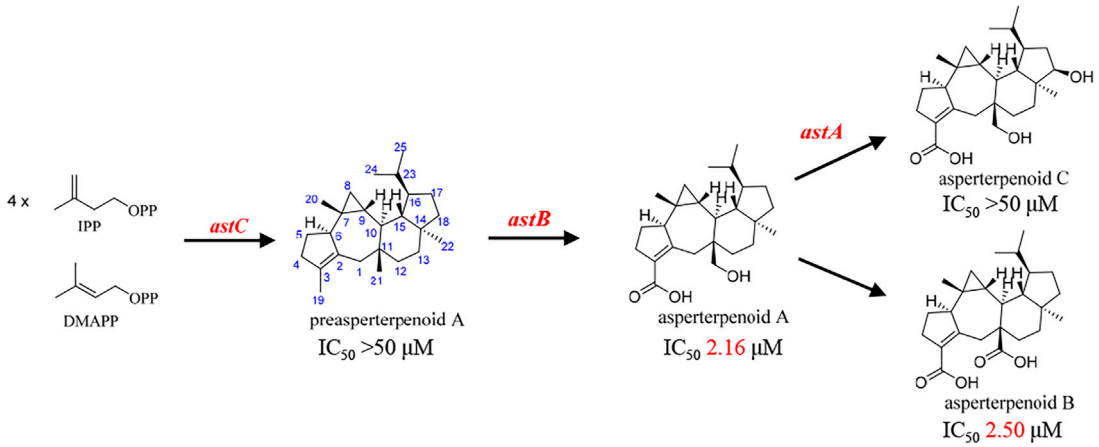

FIGURE 1 | Biosynthesis and IC_{50} value (*m*PTPB inhibitions) of the reported asperterpenoids.

(0.1% formic acid)-MeCN (0.1% formic acid) in 25 min followed by 100% MeCN (0.1% formic acid) for 35 min at 1 ml min^{-1}. The semi-preparative HPLC was performed on an Ultimate 3000 HPLC system (Thermo Fisher) with a YMC-Pack ODS-A column (10.0 mm i.d. × 250 mm, 5 μm). Column chromatography (CC) was carried out on silica gels (200–300 mesh) (Qingdao Haiyang Chemical Group Corporation, Qingdao, China).

Density Functional Theory Calculation of Hydrogen Abstraction Catalyzed by AstB

The computational reaction model (105 atoms) consisted of the two parts: 1) preasperterpenoid A and 2) Cpd I [see **Figure 3**, a brief P450 enzyme including a truncated heme and a thiolate axial ligand (SH-)]. Geometries for all the stationary points, including the reactant complex (RC), product complex (PC), and transition state (TS), were fully optimized in the gas phase using the M06 method in conjugation of the SDD(Fe)/6-31G*(C, H, O, N, and S) basis set (Fukui, 1981; Hratchian and Schlegel, 2004). (For details, see **Supplementary Information S1**.)

Fungal Source, Fermentation Condition Investigation, Extraction, and Isolation of Asperterpenoid D (1)

The strain of the *A. oryzae* transformant harboring *astBC* was obtained in previous study (Huang et al., 2019). The fungal strain was inoculated into 10 ml DPY medium (2% dextrin, 1% polypeptone, 0.5% yeast extract, 0.05% $MgSO_4{\cdot}7H_2O$, 0.5% KH_2PO_4, and 0.01% adenine) and was cultured at 28°C and 200 rpm for 2 days as the seed broth. Then the broth was transferred into 15 Erlenmeyer flasks (500 ml), each containing 100 ml of fermentation medium and grown at 28°C and 200 rpm. The screening of the fermentation conditions was carried out through bifactor analysis with culture media (rice, ME, PDB, GPY, and maltose media) and fermentation days (3, 5, and 7 days for liquid media and 10, 20, and 45 days for the rice medium, respectively) as variable factors. The rice medium contained 70 g of rice and 105 ml distilled H_2O on each flask; ME medium contained 2% malt extract, 1% polypeptone, and 2% starch; PDB medium contained 20% potato and 2% dextrose; GPY medium contained 2% starch, 0.5% peptone, and 0.2% yeast extract; maltose medium contained 3% starch, 0.15% yeast extract, 0.1% $MgSO_4$, 0.25% malt extract, 0.2% KH_2PO_4, and 0.4% $CaCO_3$ (**Supplementary Figures S6–S10**). Through the screening of fermented conditions, the intermediate II (asperterpenoid D, **1**) was found in rice, GPY, PDB, ME, and maltose media, respectively (**Supplementary Figures S6–S11**, **Figure 4**). Then fermentation was carried out in 30 Erlenmeyer flasks (500 ml), each containing 100 ml of ME medium. After autoclaving at 121°C for 30 min, each flask was inoculated with 10 ml of the seed broth and cultured at 28°C and 200 rpm for 3 days.

Mycelia were harvested by filtration and extracted with acetone (2 L). The extraction was repeated for three times, and the extract was dried under reduced pressure to obtain a crude extract (4.7 g). Then the crude extract was fractionated in a dried column vacuum chromatography system filled with silica gel, using cyclohexane (100%), cyclohexane-AcOEt (98:2), cyclohexane-AcOEt (90:10), AcOEt (100%), and MeOH (100%) to obtain fractions of 126.8, 20.5, 676.3, 544.1, and 700.6 mg, respectively. The fraction eluted with cyclohexane-AcOEt (98:2) was subjected to semi-preparative HPLC, using MeCN-H_2O (90:10, v/v) containing 0.1% formic acid at a flow rate of 3 ml min^{-1} to yield asperterpenoid D (**1**) (t_R: 13.8 min, 7.9 mg).

The Preparations of Asperterpenoids E (2) and F (3)

Asperterpenoid E (IM-I, **2**) preparation: a magnetically stirred mixture of asperterpenoid D (**1**) (20 mg, 0.05 mmol) in dry THF (tetrahydrofuran) (10 ml) was treated with $LiAlH_4$ (18.89 mg, 0.50 mmol), and the ensuing gray suspension was stirred at 85°C under a balloon of nitrogen for 48 h

TABLE 1 | ^{1}H (600 MHz) and ^{13}C NMR (150 MHz) data of compounds **1–3** in $CDCl_3$.

	1		**2**		**3**	
Position	**δ_C, type**	**δ_H, (*J* in Hz)[a]**	**δ_C, type**	**δ_H, (*J* in Hz)[a]**	**δ_C, type**	**δ_H, (*J* in Hz)[a]**
1	47.9, CH_2	a: 3.57, d (13.4)	47.0, CH_2	a: 2.44, d (13.9)	41.6, CH_2	a: 2.94, d (13.7)
	—	b: 1.79, d (13.4)	—	b: 1.71, d (13.9)	—	b: 1.45, d (13.7)
2	162.1, C	—	134.7, C	—	135.6, C	—
3	126.4, C	—	140.6, C	—	140.7, C	—
4	33.1, CH_2	a: 2.63	33.7, CH_2	a: 2.48	35.5, CH_2	a: 2.63
	—	b: 2.55, br dd (16.0, 9.8)	—	b: 2.33	—	b: 2.13, ddd (15.8, 9.6, 2.6)
5	26.0, CH_2	a: 1.98, br dd (13.0, 7.5)	26.2, CH_2	a: 1.97, br dd (13.1, 7.4)	26.6, CH_2	a: 1.98. br dd (13.1, 7.2)
	—	b: 1.90, dq (13.0, 9.4)	—	b: 1.85, dq (13.0, 9.4)	—	b: 1.86, dq (13.1, 9.4)
6	56.8, CH	2.30, br d (8.7)	54.6, CH	2.17, br d (9.0)	55.4, CH	2.18, br d (8.8)
7	21.5, C	—	22.1, C	—	22.6, C	—
8	25.5, CH_2	a: 0.61, dd (8.4, 4.2)	25.1, CH_2	a: 0.55, dd (8.3, 4.2)	25.8, CH_2	a: 0.60, dd (8.4, 4.3)
	—	b: 0.37, br t (4.7)	—	b: 0.33, dd (5.2, 4.2)	—	b: 0.33, br t (4.9)
9	29.8, CH	0.22	29.4, CH	0.10	29.1, CH	0.06, ddd (10.5, 8.4, 5.6)
10	47.7, CH	1.21	47.2, CH	1.19	47.7, CH	1.34, t (11.1)
11	40.4, C	—	39.2, C	—	43.9, C	—
12	39.3, CH_2	a: 1.61	39.3, CH_2	a: 1.60	30.0, CH_2	a: 1.91
	—	b: 1.39	—	b: 1.33	—	b: 1.24
13	35.9, CH_2	a: 1.40	35.9, CH_2	a: 1.45	35.7, CH_2	a: 1.47
	—	b: 1.31	—	b: 1.31	—	b: 1.27
14	43.0, C	—	42.9, C	—	42.8, C	—
15	50.9, CH	1.21	51.0, CH	1.19	51.4, CH	1.16, t (11.0)
16	45.4, CH	1.77	45.3, CH	1.76	45.6, CH	1.73, tdd (10.5, 4.3, 3.1)
17	22.4, CH_2	a: 1.60	22.2, CH_2	a: 1.61	22.2, CH_2	a: 1.60
	—	b: 1.45	—	b: 1.45	—	b: 1.44
18	40.1, CH_2	a: 1.37	40.0, CH_2	a: 1.35	39.9, CH_2	a: 1.37
	—	b: 1.00	—	b: 0.99	—	b: 1.00
19	171.6, C	—	59.0, CH_2	a: 4.25, d (11.1)	59.2, CH_2	a: 4.40, d (12.5)
	—	—	—	b: 4.17, d (11.1)	—	b: 3.98, d (12.5)
20	20.8, CH_3	0.93, s	20.7, CH_3	0.85, s	21.0, CH_3	0.95, s
21	20.1, CH_3	0.94, s	20.4, CH_3	0.90, s	61.3, CH_2	a: 3.69, d (10.9)
	—	—	—	—	—	b: 3.62, d (10.9)
22	17.8, CH_3	0.74, s	17.6, CH_3	0.73, s	17.7, CH_3	0.76, s
23	28.5, CH	2.30	28.4, CH	2.33	28.3, CH	2.27
24	23.3, CH_3	0.86, d (6.6)	23.2, CH_3	0.86, d (6.6)	23.1, CH_3	0.85, d (6.9)
25	15.3, CH_3	0.78, d (6.6)	15.1, CH_3	0.76, d (6.6)	15.0, CH_3	0.74, d (6.9)

[a]*Indiscernible signals from overlap or the complex multiplicity are reported without designating multiplicity.*

then extracted with water/ethyl acetate. The organic layer was concentrated under reduced pressure, and the residue was isolated by semi-preparative HPLC (YMC-Pack ODS-A column, 3 ml min^{-1}) with isocratic elution of 85% MeCN-H_2O containing 0.1% formic acid to yield **2** (t_R: 62.0 min, 5.0 mg).

Asperterpenoid F (IM-IV, **3**) preparation: A magnetically stirred mixture of asperterpenoid A (40 mg, 0.10 mmol) in dry THF (10 ml) was treated with $LiAlH_4$ (36.22 mg, 0.96 mmol), and the ensuing gray suspension was stirred at 85°C under a balloon of nitrogen for 48 h then extracted with water/ethyl acetate. The organic layer was concentrated under reduced pressure, and the residue was isolated by semi-preparative HPLC (YMC-Pack ODS-A column, 3 ml min^{-1}) with isocratic elution of 85% MeCN-H_2O containing 0.1% formic acid to yield **3** (t_R: 27.0 min, 17.7 mg).

Structural Characterizations of 1–3

Asperterpenoid D (**1**): amorphous white powder; ^{1}H and ^{13}C NMR (see **Table 1**); $[\alpha]_D^{24}$ +85.5 (*c* 0.20, MeOH); UV (MeOH) λ_{max} (log ε) 203 (3.79) and 235 (3.96); ECD λ_{nm} ($\Delta\varepsilon$) (MeOH) 211 (+1.46) and 243 (−2.84) nm; IR (KBr) ν_{max} 3,278, 3,049, 2,956, 2,927, 2,870, 2,837, 1,740, 1,679, 1,629, 1,458, 1,383, 1,287, 1,267, 948, and 936 cm^{-1}; HRESIMS (positive) *m/z* 371.2934 $[M + H]^+$ (calcd. for $C_{25}H_{39}O_2$, 371.2950) (**Supplementary Table S2**, **Supplementary Figures S14–S23**).

Asperterpenoid E (**2**): amorphous white powder; ^{1}H and ^{13}C NMR (see **Table 1**); $[\alpha]_D^{24}$ +64.0 (*c* 0.20, MeOH); UV (MeOH) λ_{max} (log ε) 203 (4.03) and 252 (4.27); ECD λ_{nm} ($\Delta\varepsilon$) (MeOH) 208 (+2.19), 236 (−0.35), 263 (+4.08), and 330 (−1.60) nm; IR (KBr) ν_{max} 3,411, 2,955, 2,927, 2,871, 2,855, 1,704, 1,602, 1,460, and 1,384 cm^{-1}; HRESIMS (positive) *m/z* 339.3036 $[M + H–H_2O]^+$ (calcd. for $C_{25}H_{39}$, 339.3046). (**Supplementary Table S4**, **Supplementary Figures S26–S35**).

Asperterpenoid F (**3**): amorphous white powder; ^{1}H and ^{13}C NMR (see **Table 1**); $[\alpha]_D^{24}$ +36.5 (*c* 0.23, MeOH); UV (MeOH) λ_{max} (log ε) 208 (3.17) and 257 (3.59); ECD λ_{nm} ($\Delta\varepsilon$) (MeOH) 207 (+2.76), 233 (−0.03), 261 (+0.96), and 338 (−0.43) nm; IR (KBr) ν_{max} 3,316, 2,953, 2,930, 2,890, 1,672, 1,461, 1,379, and 1,023 cm^{-1}; HRESIMS (positive) *m/z* 395.2917 $[M + Na]^+$ (calcd. for $C_{25}H_{40}O_2Na$, 395.2921) (**Supplementary Table S5**, **Supplementary Figures S36–S45**).

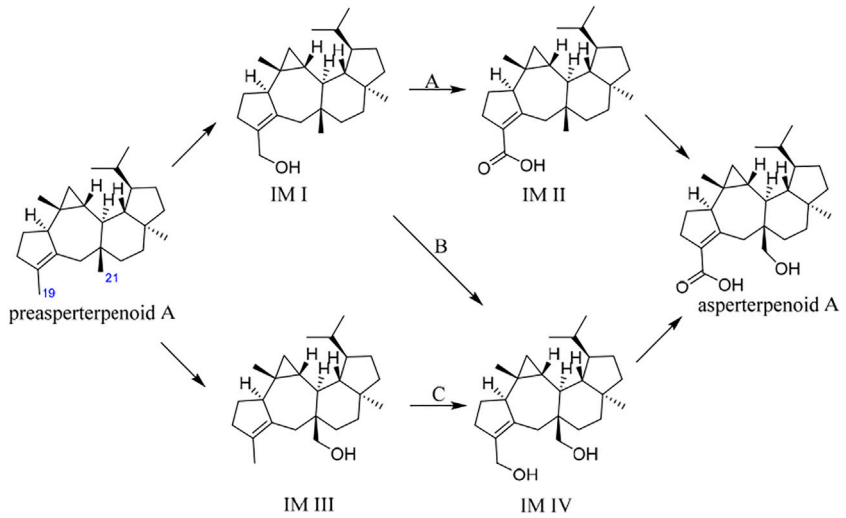

FIGURE 2 | Three possible routes for AstB enzyme catalyzing oxidations.

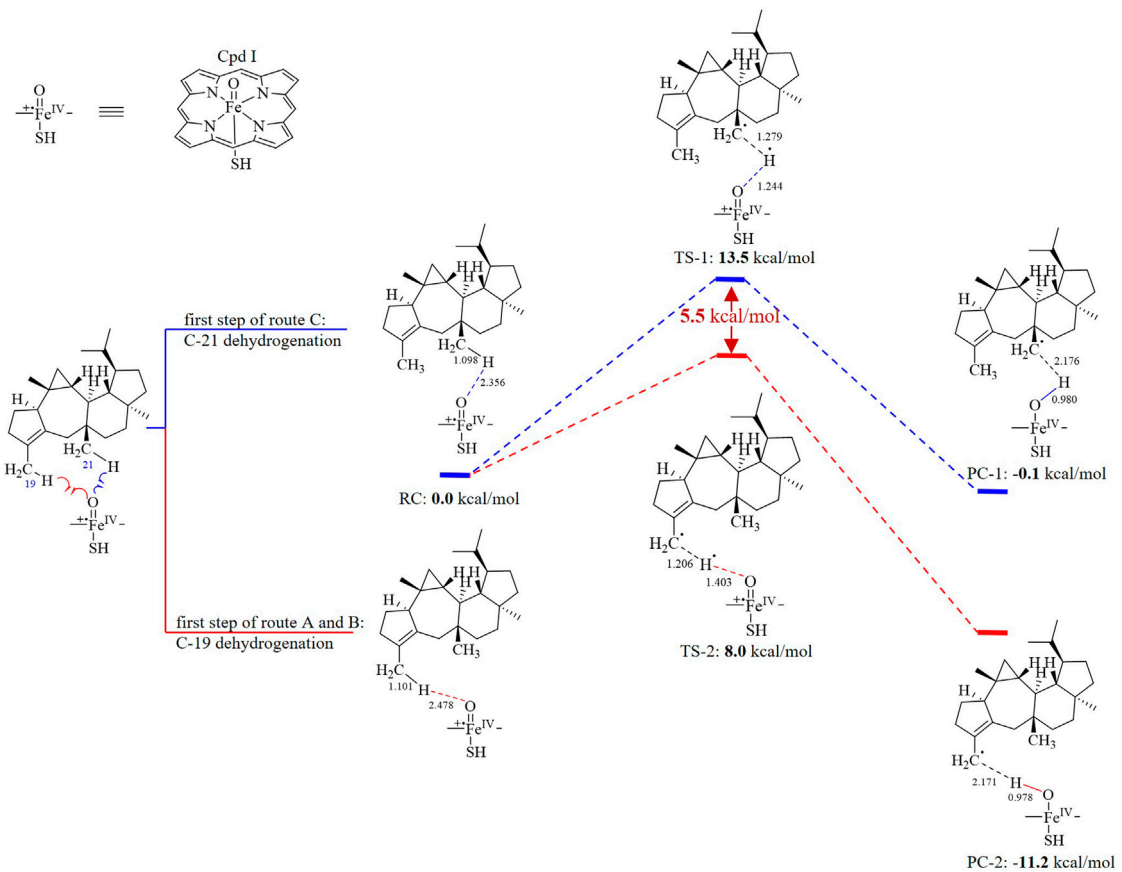

FIGURE 3 | Dehydrogenation energy calculations of C-19 dehydrogenation (first step of route A and B) and C-21 dehydrogenation (first step of route C).

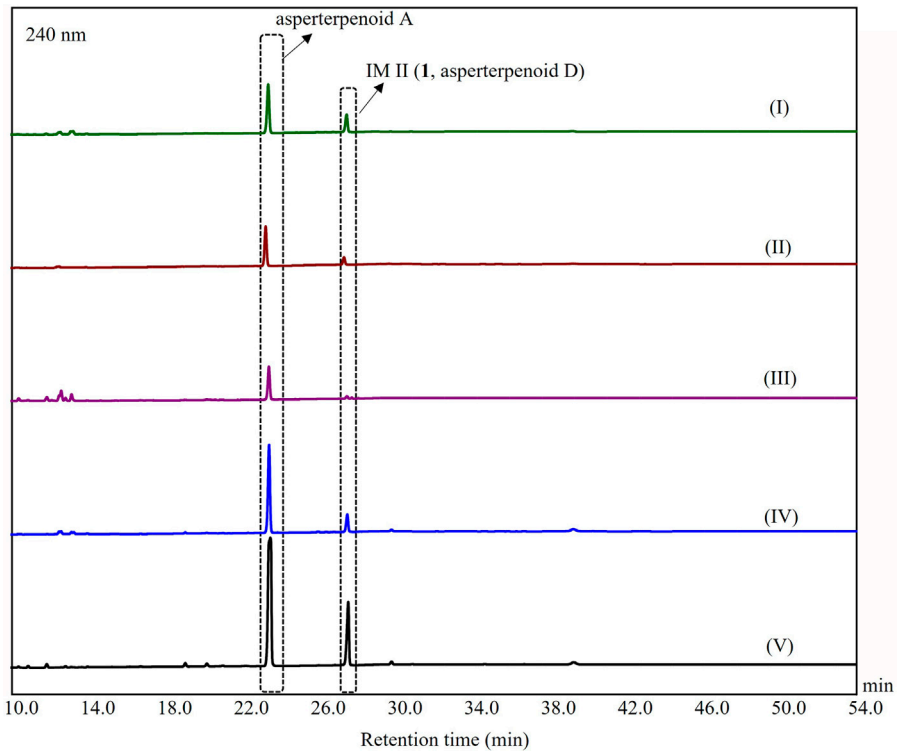

FIGURE 4 | HPLC analysis of metabolites from *A. oryzae* transformants harboring *astBC*. (I) The strain was cultured in the GPY medium for 3 days, (II) the strain was cultured in the PDB medium for 3 days, (III) the strain was cultured in the rice medium for 10 days, (IV) the strain was cultured in the maltose medium for 3 days, and (V) the strain was cultured in the ME medium for 3 days.

RESULTS AND DISCUSSION

It is known that hydroxymethyl is a common intermediate in oxidation of a methyl group to carboxyl, such as 12-OH-(-)-JAMe (the intermediate derived from (-)-JAMe) as the key intermediate in the generation of 12-COOH-(-)-JAMe (Kombrink, 2012). Because the oxidation orders of 3- and 11-methyls to hydroxymethyls and 3-hydroxymethyl to 3-carboxyl are unclear, there would be four potential intermediates, leading to three possible oxidation routes (A, B, and C) for the generation of asperterpenoid A from preasperterpenoid A catalyzed by AstB (**Figure 2**).

To the best of our knowledge, the hydrogen atoms of allyl carbons are generally more active and easier to leave than those of other kinds of carbons (Zerth et al., 2003). Based on this, it is proposed that the route A would exist in the transformation of preasperterpenoid A to asperterpenoid A catalyzed by AstB because C-19 (allyl carbon) oxidation is theoretically prior to C-21 oxidation in the route A. In order to confirm this inference, the DFT calculations were carried out (Denningtonll TK et al., 2003; Frisch GWT et al., 2013; Fukui, 1981; Hratchian and Schlegel, 2004; Sansen et al., 2007; Tao et al., 2015).

The oxidation first occurring at C-19 or C-21 is decided by the Gibbs free energy barriers of C-19 and C-21 dehydrogenations. Based on the DFT calculations (**Figure 3**), the free energy barriers of C-19 (transition state 2, TS-2) and C-21 (transition state 1, TS-1) dehydrogenations were predicted to be 8.0 and 13.5 kcal/mol, respectively. Therefore, the energy gap of two dehydrogenations was 5.5 kcal/mol (the probability of the occurrence of C-19 dehydrogenation was 99.99%), which indicated that C-19 oxidation would be the first step in the oxidations catalyzed by AstB. The calculation results also confirmed that the hydrogen atoms of allyl carbons are easier to leave than those of other kinds of carbons. In addition, H-19 in IM I would be easier to leave rather than H-21 because of the inductive effect from 19-hydroxyl group. Therefore, the 3-hydroxymethyl group of IM I would be subsequently oxidized to form IM II, rather than to form IM IV. These results were consistent with our inference that the route A would exist in the oxidations of AstB. (For details, see **Supplementary Information S1**).

In order to confirm the results from the DFT calculations, the acquirement of the key intermediates was necessary. In our previous study, no intermediate was observed in the extract of the heterologous expressed *astBC*-harboring transformant strain (*A. oryzae*), which would be resulted from the fermentation without an appropriate condition or the trace amount of the intermediates (Huang et al., 2019). According to this, the screening of the fermentation conditions was carried out using a bifactor analysis with a culture medium (rice, GPY, PDB, ME, and maltose media) and fermentation days (3, 5, and 7 days for liquid media and 10, 20, and 45 days for rice medium) as variable factors. (For details, see **Supplementary Information S2**, **Supplementary Figures**

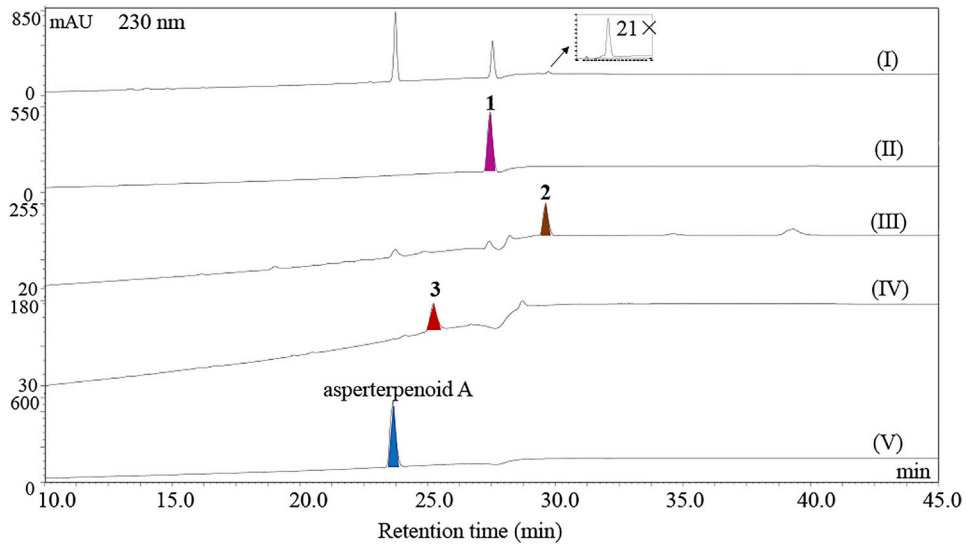

FIGURE 5 | HPLC analysis of metabolites. (I) HPLC chromatogram of the extract of the *A. oryzae* transformants harboring *astBC* cultured in the ME medium for 3 days, (II–V) HPLC chromatograms of asperterpenoid D (**1**), asperterpenoid E (**2**), asperterpenoid F (**3**), and asperterpenoid A.

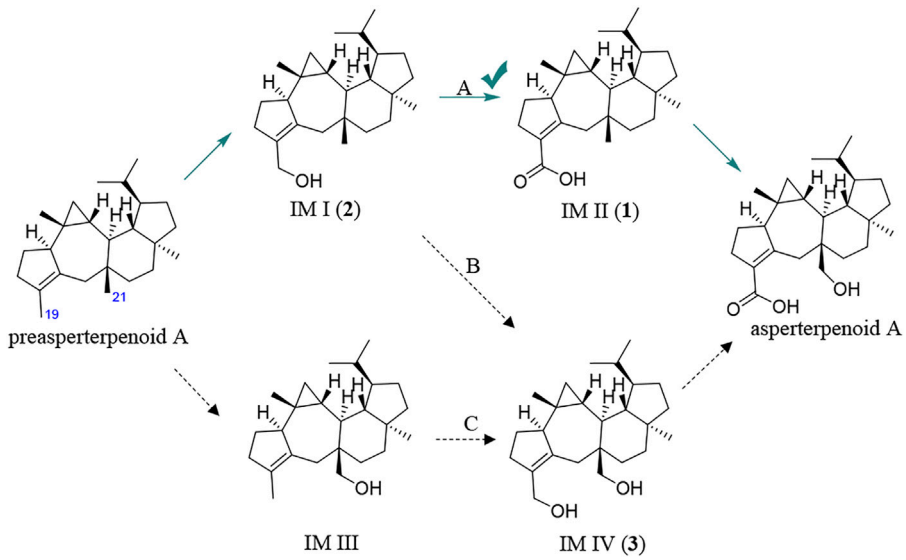

FIGURE 6 | Main pathway for AstB enzyme catalyzing oxidations.

S6–S10.) An additional chromatographic peak was observed when the strain was fermented with rice, GPY, PDB, maltose, and ME media, respectively. Among them, the peak in the extract of the fermentation using ME medium with 3 days was the most obvious (**Figure 4**). The HPLC-MS analysis showed that the peak would be a new asperterpenoid (the positive ion peak at *m/z* 353.39 $[M + H - H_2O]^+$) (**Supplementary Figure S11**). After the isolation of this additional chromatographic peak through the large-scale fermentation with the ME medium for 3 days, the peak compound (**1**) was obtained. Based on the detailed NMR analysis (**Supplementary Table S2**, **Supplementary Figures S18–S23**) combined with ECD calculation (**Supplementary Information S4.2**, **Supplementary Figures S24, S25**), the structure of **1** was determined as a new asperterpenoid with 3-methyl oxidized to 3-carboxyl, which was IM II in route A and named as asperterpenoid D. The result confirmed the existence of route A in the oxidations catalyzed by AstB.

Furthermore, the potential intermediates IM I and IM IV were prepared with the artificial reduction from

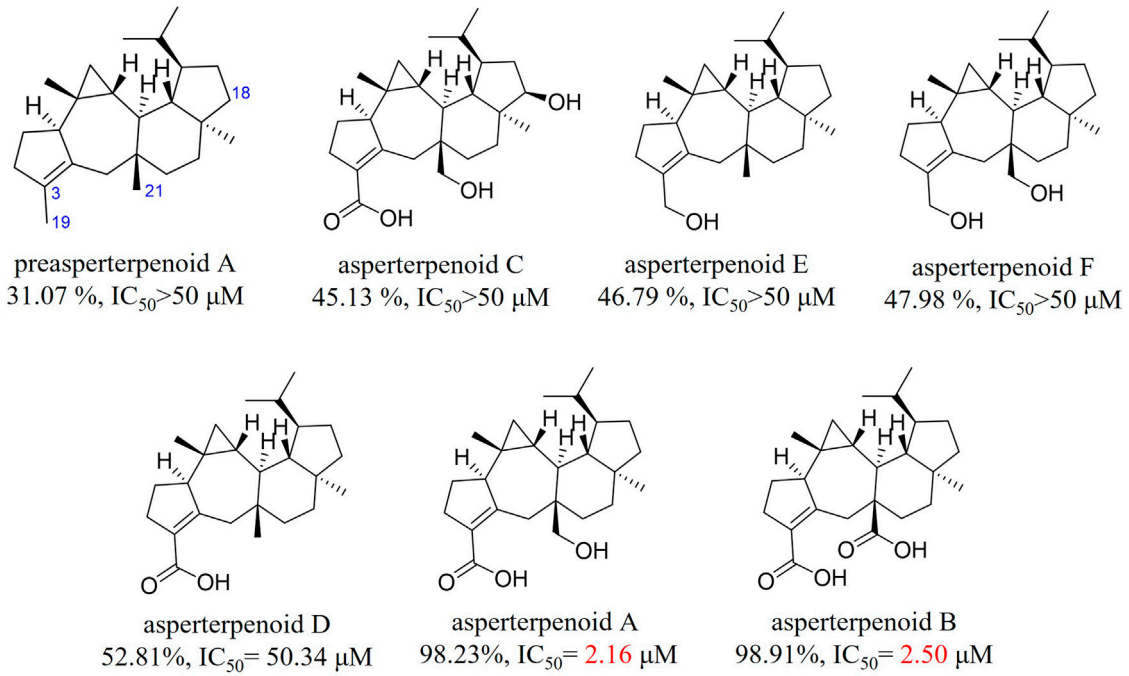

FIGURE 7 | *m*PTPB inhibition at 50 μM and IC_{50} value of asperterpenoids.

asperterpenoid D and asperterpenoid A because the potential intermediates IM I and IM IV were the biosynthetic precursors of asperterpenoid D and asperterpenoid A in the relevant proposed route. After reduction from asperterpenoid D with $LiAlH_4$, the potential intermediate IM I (**2**, named asperterpenoid E) was obtained, and its structure was confirmed as a new asperterpenoid with 3-methyl oxidized to 3-methylol based the detailed analyses of NMR data (**Supplementary Table S4**, **Supplementary Figures S26–S35**). By the same way, the potential intermediate IM IV (**3**, named asperterpenoid F) was also obtained, and its structure was identified by the detailed analyses of NMR (**Supplementary Table S5**, **Supplementary Figures S36–S45**). Through HPLC-MS analysis with compounds **1–3** and asperterpenoid A as standards (HPLC analysis see **Figure 5**, HPLC-MS analysis see **Supplementary Figures S12, S13**), a tiny chromatographic peak (t_R = 29.6 min) was identified as asperterpenoid E (**2**) in the HPLC chromatogram of the *astBC*-harboring transformant strain (*A. oryzae*) in the ME medium cultured for 3 days (see **Figure 5I**, **Supplementary Information S3**, **Supplementary Figure S12**). In the HPLC-MS analysis, however, there was no peak with the same retention time and ion peak as asperterpenoid F (**3**) in the extract of the *astBC*-harboring transformant strain (*A. oryzae*) (see **Supplementary Figure S13**), indicating that **3** would not exist. These experiment data supported that the route A was the oxidization cascade of AstB (**Figure 6**).

In the previous study, it was found that asperterpenoids A and B showed potent inhibition against *m*PTPB and 18-hydroxyl would weaken the inhibition (Huang et al., 2019). For the abstention of asperterpenoids with 3-hydroxymethyl, the relationship between the oxidation stations of C-19 and C-21 in asperterpenoids and their *m*PTPB inhibition was unknown. In this research, the *m*PTPB inhibition of three new asperterpenoids (**1–3**, asperterpenoids D–F) and five known asperterpenoids (preasperterpenoid A and asperterpenoids A–C) was evaluated (**Figure 7**, detail see **Supplementary Information S7**, **Supplementary Table S6**). Among these new asperterpenoids, only asperterpenoid D (**2**) presented the *m*PTPB inhibition (IC_{50} = 50.34 μM), which was weaker than those of asperterpenoids A and B. The data clearly showed that 3-carboxyl and the oxidation station of C-21 were essential for *m*PTPB inhibition of asperterpenoids.

In conclusion, the oxidation cascade of a rare multifunctional P450 enzyme (AstB) was cleared based on the combination of the quantum chemistry calculations and the experiments of obtaining the potential intermediates and the HPLC-MS detection of the potential intermediates. Furthermore, the relationship between the oxidation stations of C-19 and C-21 in asperterpenoids and their *m*PTPB inhibition was also revealed.

DATA AVAILABILITY STATEMENT

The original contributions presented in the study are included in the article/**Supplementary Material**; further inquiries can be directed to the corresponding authors.

AUTHOR CONTRIBUTIONS

This study was designed and supported by HG, X-SY, and G-DC. The isolations, structural elucidations, calculated ECD, and the fungal fermentation were performed by H-YH and J-HH. Density functional theory (DFT) calculation of hydrogen abstraction catalyzed by AstB was performed by H-YH and Y-HW. The anti-*m*PTPB assay was performed by Y-JL and Z-GS. The transformant strains were supplied by J-HH and DH. The manuscript was written by H-YH and G-DC. The paper was revised by HG.

FUNDING

This work was financially supported by grants from National Key Research and Development Program of China (2018YFA0903200/2018YFA0903201), the National Natural Science Foundation of China (81925037 and 81973213), National High-level Personnel of Special Support Program (2017RA2259), the 111 Project of Ministry of Education of the People's Republic of China (B13038), Guangdong Natural Science Funds for Distinguished Young Scholar (2017A03036027, China), Local Innovative and Research Teams Project of Guangdong Pearl River Talents Program (2017BT01Y036, China), and K. C. Wong Education Foundation (G-DC, 2021, China). The calculations were supported by the high-performance computing platform of Jinan University.

SUPPLEMENTARY MATERIAL

The Supplementary Material for this article can be found online at: https://www.frontiersin.org/articles/10.3389/fchem.2021.785431/full#supplementary-material

REFERENCES

Bai, X. B., Guo, H., Chen, D. D., Yang, Q., Tao, J., and Liu, W. (2020). Isolation and Structure Determination of Two New Nosiheptide-Type Compounds Provide Insights into the Function of the Cytochrome P450 Oxygenase NocV in Nocathiacin Biosynthesis. *Org. Chem. Front.* 7, 584–589. doi:10.1039/c9qo01328h

Bertram, G. K., Susan, B. M., and Anthony, J. T. (2012). *Basic & Clinic Pharmacology*. New York, NY: McGraw Hill.

Child, S. A., Rossi, V. P., and Bell, S. G. (2019). Selective ω-1 Oxidation of Fatty Acids by CYP147G1 from *Mycobacterium marinum*. *Biochim. Biophys. Acta (Bba) - Gen. Subjects* 1863, 408–417. doi:10.1016/j.bbagen.2018.11.013

Cochrane, R. V. K., and Vederas, J. C. (2014). Highly Selective but Multifunctional Oxygenases in Secondary Metabolism. *Acc. Chem. Res.* 47, 3148–3161. doi:10.1021/ar500242c

Denningtonll TK, R., Millam, J., Eppinnett, K., Hovell, W. L., and Gilliland, R. (2003). *Gauss View*. version 3.0. Wallingford, CT: Gaussian Inc.

Erickson, D. A., Hollfelder, S., Tenge, J., Gohdes, M., Burkhardt, J. J., and Krieter, P. A. (2007). *In Vitro* metabolism of the Analgesic Bicifadine in the Mouse, Rat, Monkey, and Human. *Drug Metab. Dispos.* 35, 2232–2241. doi:10.1124/dmd.107.016055

Frisch GWT, M. J., Schlegel, H. B., Scuseria, G. E., Robb, M. A., Cheeseman, J. R., Scalmani, G., et al. (2013). *Gaussian 09, Revisin D01*. Wallingford, CT: Gaussian Inc.

Fukui, k. (1981). The Path of Chemical Reactions - The IRC Approach. *Acc. Chem. Res.* 14, 363–368. doi:10.1021/ar00072a001

Hratchian, H. P., and Schlegel, H. B. (2004). Accurate Reaction Paths Using a Hessian Based Predictor-Corrector Integrator. *J. Chem. Phys.* 120, 9918–9924. doi:10.1063/1.1724823

Huang, J.-H., Lv, J.-M., Wang, Q.-Z., Zou, J., Lu, Y.-J., Wang, Q.-L., et al. (2019). Biosynthesis of an Anti- Tuberculosis Sesterterpenoid Asperterpenoid A. *Org. Biomol. Chem.* 17, 248–251. doi:10.1039/c8ob02832j

Huang, X.-S., Huang, H.-B., Li, H.-X., Sun, X.-F., Huang, H.-R., Lu, Y.-J., et al. (2013). Asperterpenoid A, a New Sesterterpenoid as an Inhibitor of mycobacterium Tuberculosis Protein Tyrosine Phosphatase B from the Culture of *Aspergillus* sp. 16-5c. *Org. Lett.* 15, 721–723. doi:10.1021/ol303549c

Jiang, F.-L., Gong, T., Chen, J.-J., Chen, T.-J., Yang, J.-L., and Zhu, P. (2021). Synthetic Biology of Plants-Derived Medicinal Natural Products. *Chin. J. Biotechnol.* 37, 1931–1951. doi:10.13345/j.cjb.210138

Keyler, D., Pentel, P. R., Kuehl, G., Collins, G., and Murphy, S. E. (2003). Effects of Nicotine Infusion on the Metabolism of the Tobacco Carcinogen 4-(methylnitrosamino)-1-(3-Pyridyl)-L-Butanone (NNK) in Rats. *Cancer Lett.* 202, 1–9. doi:10.1016/j.canlet.2003.07.004

Kombrink, E. (2012). Chemical and Genetic Exploration of Jasmonate Biosynthesis and Signaling Paths. *Planta* 236, 1351–1366. doi:10.1007/s00425-012-1705-z

Kramlinger, V. M., Rojas, M. A., Kanamori, T., and Guengerich, F. P. (2015). Cytochrome P450 3A Enzymes Catalyze the O-6-Demethylation of Thebaine, a Key Step in Endogenous Mammalian Morphine Biosynthesis. *J. Biol. Chem.* 290, 20200–20210. doi:10.1074/jbc.M115.665331

Lin, H. C., Hewage, R. T., Lu, Y. C., and Chooi, Y. H. (2019). Biosynthesis of Bioactive Natural Products from Basidiomycota. *Org. Biomol. Chem.* 17, 1027–1036. doi:10.1039/c8ob02774a

Long, L., and Dolan, M. E. (2001). Role of Cytochrome P450 Isoenzymes in Metabolism of O-6-Benzylguanine: Implications for Dacarbazine Activation. *Clin. Cancer Res.* 7, 4239–4244.

Mendez, C., Baginsky, C., Hedden, P., Gong, F., Caru, M., and Rojas, M. C. (2014). Gibberellin Oxidase Activities in *Bradyrhizobium japonicum* Bacteroids. *Phytochemistry* 98, 101–109. doi:10.1016/j.phytochem.2013.11.013

Moses, T., Pollier, J., Faizal, A., Apers, S., Pieters, L., Thevelein, J. M., et al. (2015). Unraveling the Triterpenoid Saponin Biosynthesis of the African Shrub *Maesa lanceolata*. *Mol. Plant* 8, 122–135. doi:10.1016/j.molp.2014.11.004

Narita, K., Chiba, R., Minami, A., Kodama, M., Fujii, I., Gomi, K., et al. (2016). Multiple Oxidative Modifications in the Ophiobolin Biosynthesis: P450 Oxidations Found in Genome Mining. *Org. Lett.* 18, 1980–1983. doi:10.1021/acs.orglett.6b00552

Peyronneau, M. A., Saba, W., Dolle, F., Goutal, S., Coulon, C., Bottlaender, M., et al. (2012). Difficulties in Dopamine Transporter Radioligand PET Analysis: the Example of LBT-999 Using [F-18] and [C-11] Labelling Part II: Metabolism Studies. *Nucl. Med. Biol.* 39, 347–359. doi:10.1016/j.nucmedbio.2011.09.006

Sansen, S., Yano, J. K., Reynald, R. L., Schoch, G. A., Griffin, K. J., Stout, C. D., et al. (2007). Adaptations for the Oxidation of Polycyclic Aromatic Hydrocarbons Exhibited by the Structure of Human P450 1a2. *J. Biol. Chem.* 282, 14348–14355. doi:10.1074/jbc.M611692200

Sheng, X., Zhang, H.-M., Hollenberg, P. F., and Newcomb, M. (2009). Kinetic Isotope Effects in Hydroxylation Reactions Effected by Cytochrome P450 Compounds I Implicate Multiple Electrophilic Oxidants for P450-Catalyzed Oxidations. *Biochem* 48, 1620–1627. doi:10.1021/bi802279d

Tao, J., Kang, Y., Xue, Z.-Y., Wang, Y.-T., Zhang, Y., Chen, Q., et al. (2015). Theoretical Study on the N-Demethylation Mechanism of Theobromine Catalyzed by P450 Isoenzyme 1a2. *J. Mol. Graph.* 61, 123–132. doi:10.1016/j.jmgm.2015.06.017

Yanni, S. B., Annaert, P. P., Augustijns, P., Bridges, A., Gao, Y., Benjamin, D. K., et al. (2008). Role of Flavin-Containing Monooxygenase in Oxidative

Metabolism of Voriconazole by Human Liver Microsomes. *Drug Metab. Dispos.* 36, 1119–1125. doi:10.1124/dmd.107.019646

Zeng, H.-C., Yin, G.-P., Wei, Q., Li, D.-H., Wang, Y., Hu, Y.-C., et al. (2019). Unprecedented [5.5.5.6]Dioxafenestrane Ring Construction in Fungal Insecticidal Sesquiterpene Biosynthesis. *Angew. Chem. Int. Edit.* 58, 6569–6573. doi:10.1002/anie.201813722

Zerth, H. M., Leonard, N. M., Mohan, R. S., Leonard, N. M., and Mohan, R. S. (2003). Synthesis of Homoallyl Ethers via Allylation of Acetals in Ionic Liquids Catalyzed by Trimethylsilyl Trifluoromethanesulfonate. *Org. Lett.* 5, 55–57. doi:10.1021/ol0271739

Zhang, W.-Y., Zhong, Y., Yu, Y., Shi, D.-F., Huang, H.-Y., Tang, X.-L., et al. (2020). 4-Hydroxy Pyridones from Heterologous Expression and Cultivation of the Native Host. *J. Nat. Prod.* 83, 3338–3346. doi:10.1021/acs.jnatprod.0c00675

Zhou, J.-W., Hu, T.-Y., Liu, Y., Tu, L.-C., Song, Y.-D., Lu, Y., et al. (2021). Cytochrome P450 Catalyses the 29-Carboxyl Group Formation of Celastrol. *Phytochemistry* 190, 112868. doi:10.1016/j.phytochem.2021.112868

Conflict of Interest: The authors declare that the research was conducted in the absence of any commercial or financial relationships that could be construed as a potential conflict of interest.

Publisher's Note: All claims expressed in this article are solely those of the authors and do not necessarily represent those of their affiliated organizations, or those of the publisher, the editors, and the reviewers. Any product that may be evaluated in this article, or claim that may be made by its manufacturer, is not guaranteed or endorsed by the publisher.